Supplementary Figures

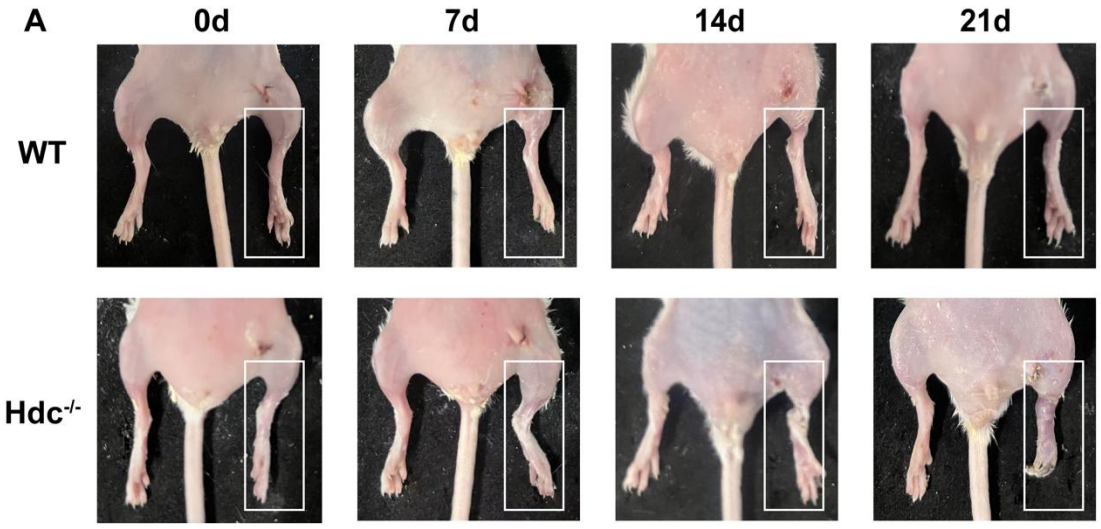

Fig. S1. The Deletion of Hdc Impairs Hindlimb Ischemia (HLI)-Induced Revascularization. **(A)** A picture of the ischemic limb is shown at each point per group. Each photograph was taken under the same conditions (n=6).

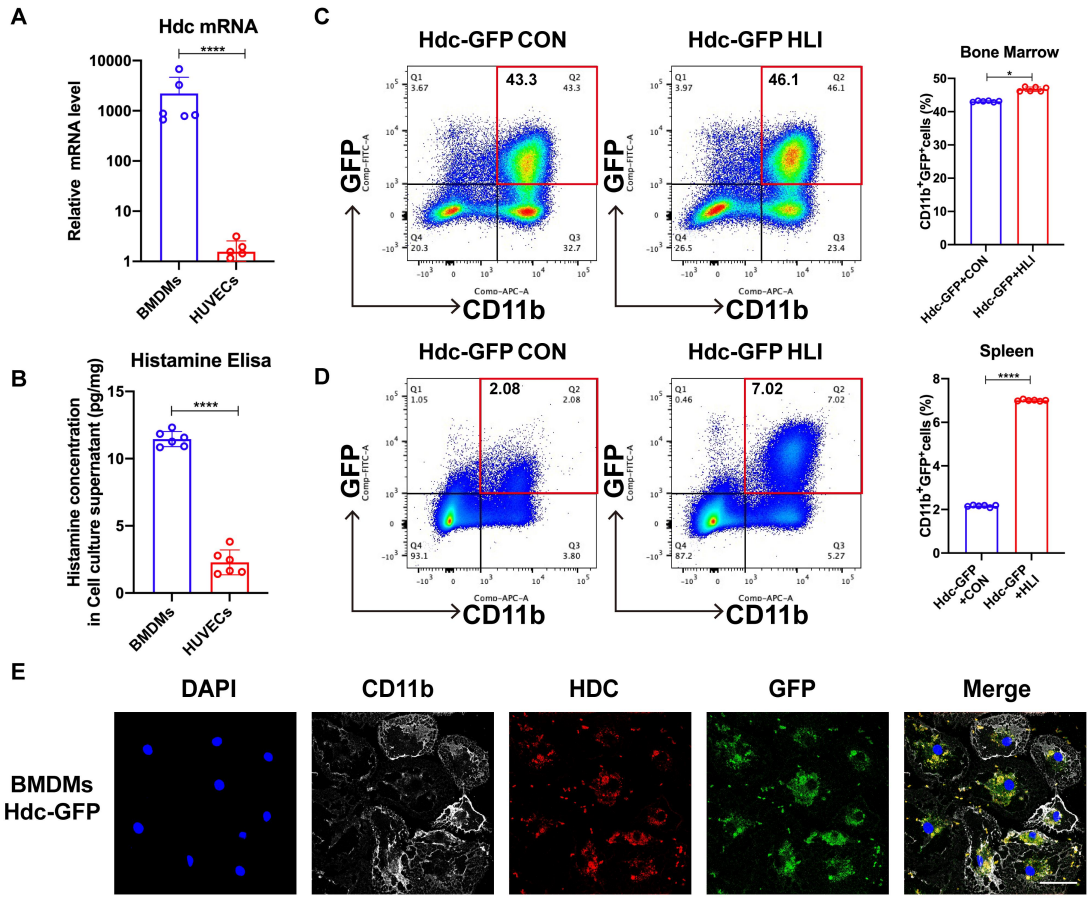

Fig. S2. Bone marrow-derived macrophages (BMDMs) are the predominant HDC-expressing sites during HLI. (A) RT-qPCR showing mRNA levels of HDC mRNA in BMDMs and HUVECs (n=6). **(B)** ELISA of secreted Histamine from BMDMs and HUVECs (n=6). **(C)** Representative images and quantification of FACS analysis of the GFP^+ cell percentage in the bone marrow of Hdc-GFP^+ mice before and 3 days after HLI (n=6). **(D)** Representative images and quantification of FACS analysis of the GFP^+ cell percentage in the spleen of Hdc-GFP^+ mice before and 3 days after HLI (n=6). **(E)** Representative images of HDC (red), GFP (green), CD11b (white) and DAPI (blue) immunostainings of bone marrow derived macrophages of Hdc-GFP^+ mice; Scale bar, 20μm. For all experiments, error bars represent the mean ± SD. *P < 0.05, **P < 0.01, ***P < 0.001, ****P < 0.0001

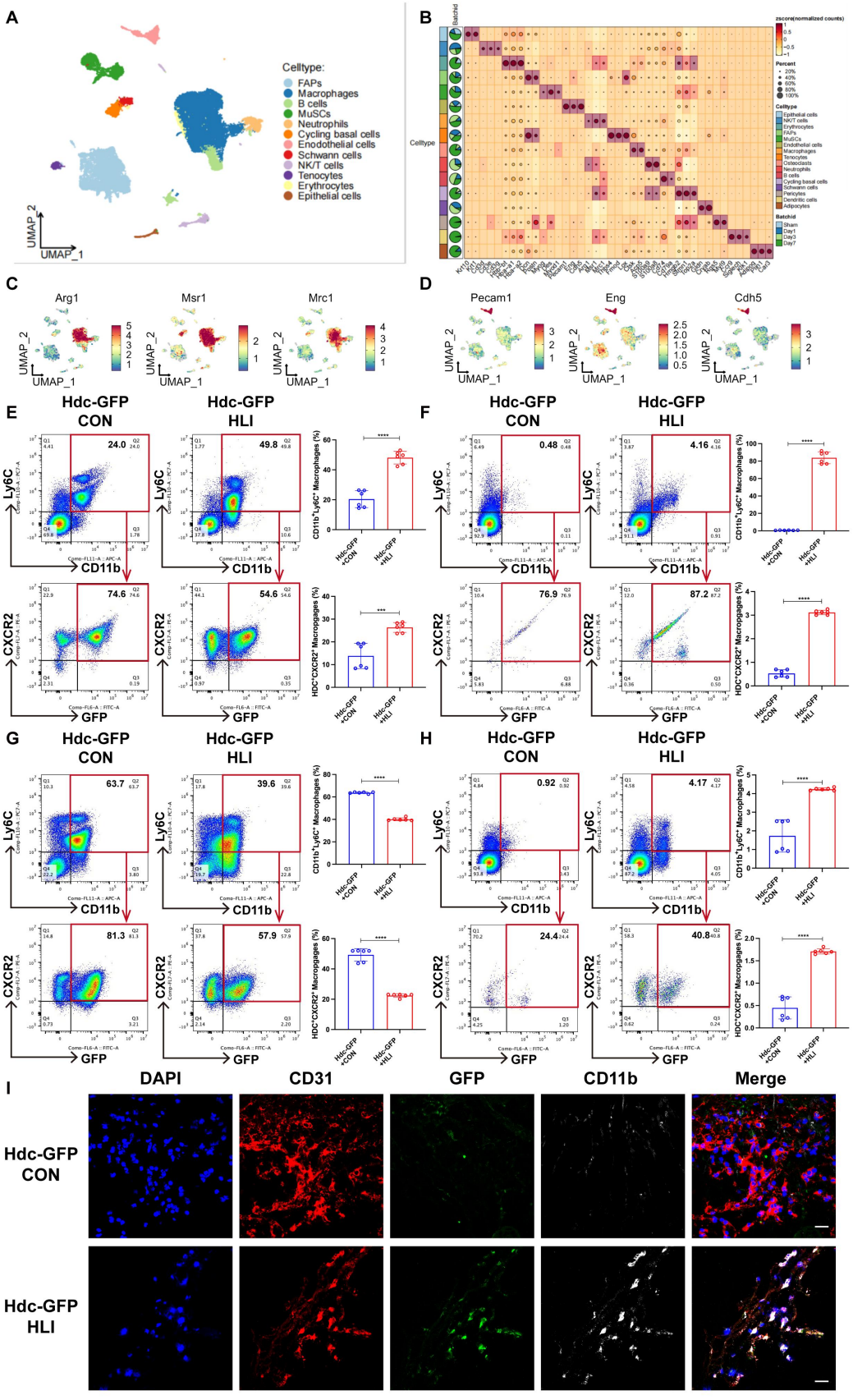
A
Celltype:
FAPs
Macrophages
B cells
MuSCs
Neutrophils
Cycling basal cells
Endothelial cells
Schwann cells
NK/T cells
Tenocytes
Erythrocytes
Epithelial cells
UMAP_2
UMAP_1
B
Batchid
Celltype
zscore(normalized counts)
Percent
Celltype
Batchid
Sham
Day1
Day3
Day7
C
Arg1
Msr1
Mrc1
D
Pecam1
Eng
Cdh5
E
Hdc-GFP CON
Hdc-GFP HLI
Ly6C
CD11b
CXCR2
GFP
CD11b+Ly6C+ Macrophages (%)
HDC+CXCR2+ Macrophages (%)
F
Hdc-GFP CON
Hdc-GFP HLI
G
Hdc-GFP CON
Hdc-GFP HLI
H
Hdc-GFP CON
Hdc-GFP HLI
I
DAPI
CD31
GFP
CD11b
Merge
Hdc-GFP CON
Hdc-GFP HLI

1

Fig. S3. Single-cell transcriptomics analysis suggests an association between HDC$^+$ macrophages and angiogenesis during the process of HLI (A) Reference-based integration of skeletal muscle mononucleated cell datasets prepared from WT mice (GSE227075). **(B)** Dot plot of selected marker genes for each cluster and lineage in aggregate cell clusters. **(C)** Feature plot showing Arg1, Msr1, and Mrc1 gene expression in macrophages. **(D)** Feature plot showing Pecam1, Eng, and Cdh5 gene expression in endothelial cells. **(E)** Representative images and quantification of FACS analysis of the HDC$^+$CXCR2$^+$ cell percentage in the peripheral blood of Hdc-GFP mice before and 1 days after HLI (n=6). **(F)** Representative images and quantification of FACS analysis of the HDC$^+$CXCR2$^+$ cell percentage in the muscle tissue of Hdc-GFP mice before and 1 days after HLI (n=6). **(G)** Representative images and quantification of FACS analysis of the HDC$^+$CXCR2$^+$cell percentage in the bone marrow of Hdc-GFP$^+$ mice before and 1 days after HLI (n=6). **(H)** Representative images and quantification of FACS analysis of the HDC$^+$CXCR2$^+$cell percentage in the spleen of Hdc-GFP$^+$ mice before and 1 days after HLI (n=6). **(I)**Representative images of CD31 (red), Hdc-GFP (green), CXCR2 (White) and DAPI (blue) immunostainings of gastrocnemius muscle of Hdc-GFP mice before and 3 days after HLI; Scale bar, 50μm. For all experiments, error bars represent the mean ± SD. *P < 0.05, **P < 0.01, ***P < 0.001, ****P < 0.0001

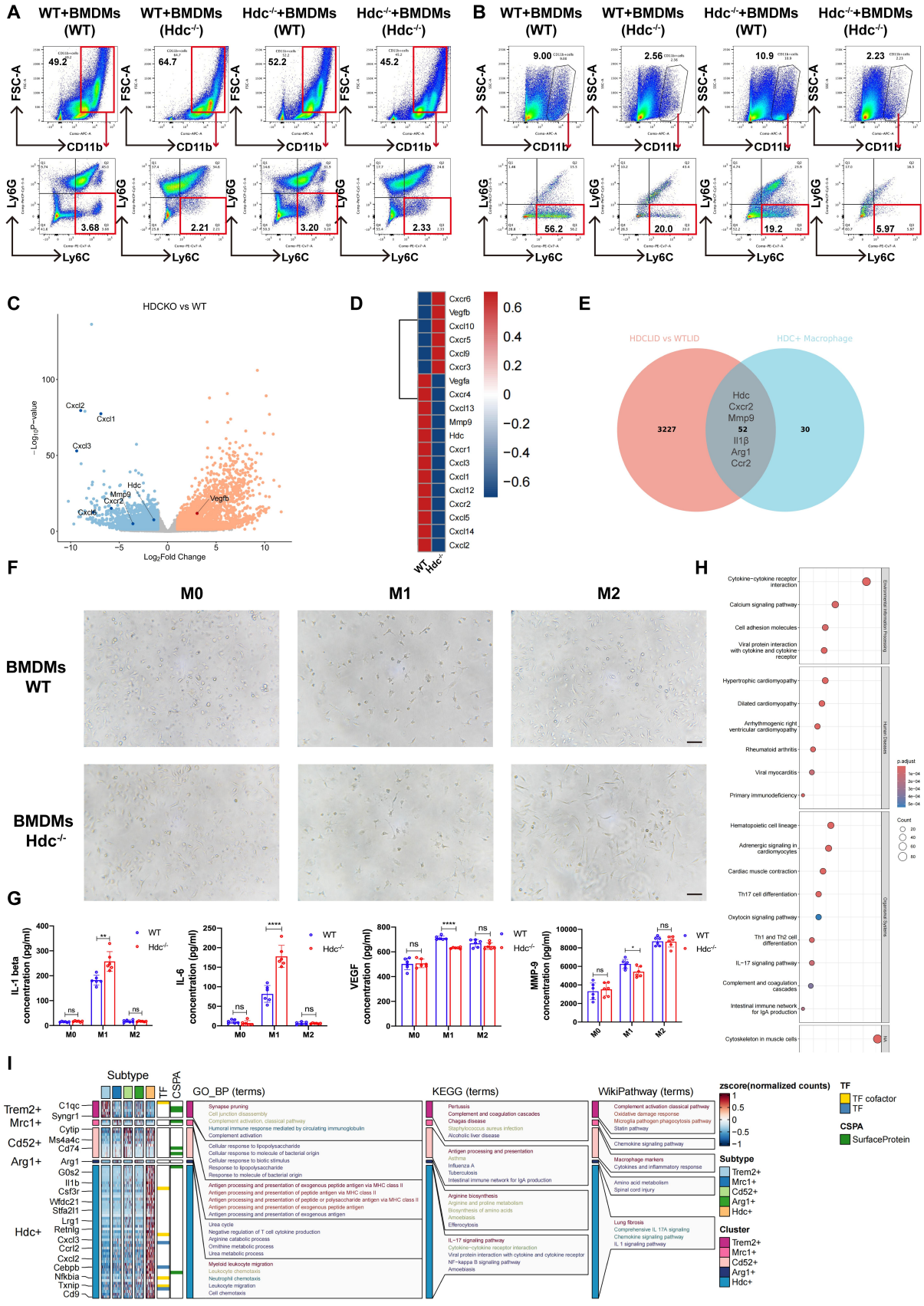
A
WT+BMDMs (WT)
WT+BMDMs (Hdc-/-)
Hdc-/-+BMDMs (WT)
Hdc-/-+BMDMs (Hdc-/-)
FSC-A
SSC-A
CD11b
Ly6G
Ly6C
49.2
64.7
52.2
45.2
3.68
2.21
3.20
2.33
B
9.00
2.56
10.9
2.23
56.2
20.0
19.2
5.97
C
HDCKO vs WT
−Log10P-value
Log2Fold Change
Cxcl2
Cxcl1
Cxcl3
Hdc
Mmp9
Cxcr2
Cxcl6
Vegfb
D
Cxcr6
Vegfb
Cxcl10
Cxcr5
Cxcl9
Cxcr3
Vegfa
Cxcr4
Cxcl13
Mmp9
Hdc
Cxcr1
Cxcl3
Cxcl1
Cxcl12
Cxcr2
Cxcl5
Cxcl14
Cxcl2
WT
Hdc-/-
E
HDCLID vs WTLID
HDC+ Macrophage
3227
52
30
Hdc
Cxcr2
Mmp9
Il1β
Arg1
Ccr2
F
M0
M1
M2
BMDMs WT
BMDMs Hdc-/-
G
IL-1 beta concentration (pg/ml)
IL-6 concentration (pg/ml)
VEGF concentration (pg/ml)
MMP-9 concentration (pg/ml)
WT
Hdc-/-
ns
H
Cytokine−cytokine receptor interaction
Calcium signaling pathway
Cell adhesion molecules
Viral protein interaction with cytokine and cytokine receptor
Hypertrophic cardiomyopathy
Dilated cardiomyopathy
Arrhythmogenic right ventricular cardiomyopathy
Rheumatoid arthritis
Viral myocarditis
Primary immunodeficiency
Hematopoietic cell lineage
Adrenergic signaling in cardiomyocytes
Cardiac muscle contraction
Th17 cell differentiation
Oxytocin signaling pathway
Th1 and Th2 cell differentiation
IL−17 signaling pathway
Complement and coagulation cascades
Intestinal immune network for IgA production
Cytoskeleton in muscle cells
Environmental Information Processing
Human Diseases
Organismal Systems
p.adjust
Count
I
Subtype
TF
CSPA
GO_BP (terms)
KEGG (terms)
WikiPathway (terms)
Trem2+
Mrc1+
Cd52+
Arg1+
Hdc+
C1qc
Syngr1
Cytip
Ms4a4c
Cd74
Arg1
G0s2
Il1b
Csf3r
Wfdc21
Stfa2l1
Lrg1
Retnlg
Cxcl3
Ccrl2
Cxcl2
Cebpb
Nfkbia
Txnip
Cd9
Synapse pruning
Cell junction disassembly
Complement activation, classical pathway
Humoral immune response mediated by circulating immunoglobulin
Complement activation
Cellular response to lipopolysaccharide
Cellular response to molecule of bacterial origin
Cellular response to biotic stimulus
Response to lipopolysaccharide
Response to molecule of bacterial origin
Antigen processing and presentation of exogenous peptide antigen via MHC class II
Antigen processing and presentation of peptide antigen via MHC class II
Antigen processing and presentation of peptide or polysaccharide antigen via MHC class II
Antigen processing and presentation of exogenous peptide antigen
Antigen processing and presentation of exogenous antigen
Urea cycle
Negative regulation of T cell cytokine production
Arginine catabolic process
Ornithine metabolic process
Urea metabolic process
Myeloid leukocyte migration
Leukocyte chemotaxis
Neutrophil chemotaxis
Leukocyte migration
Cell chemotaxis
Pertussis
Complement and coagulation cascades
Chagas disease
Staphylococcus aureus infection
Alcoholic liver disease
Antigen processing and presentation
Asthma
Influenza A
Tuberculosis
Intestinal immune network for IgA production
Arginine biosynthesis
Arginine and proline metabolism
Biosynthesis of amino acids
Amoebiasis
Efferocytosis
IL-17 signaling pathway
Cytokine−cytokine receptor interaction
Viral protein interaction with cytokine and cytokine receptor
NF−kappa B signaling pathway
Amoebiasis
Complement activation classical pathway
Oxidative damage response
Microglia pathogen phagocytosis pathway
Statin pathway
Chemokine signaling pathway
Macrophage markers
Cytokines and inflammatory response
Amino acid metabolism
Spinal cord injury
Lung fibrosis
Comprehensive IL 17A signaling
Chemokine signaling pathway
IL 1 signaling pathway
zscore(normalized counts)
Subtype
Cluster
TF cofactor
SurfaceProtein

1

Fig. S4. Hdc knockout induced atypical macrophage polarization and down-regulated pro-angiogenic factors expression during HLI by regulating NF-κB and MAPK pathways **(A)** Representative images of FACS analysis of the macrophage's percentage in the peripheral blood of WT and $Hdc^{-/-}$ mice transplanted with bone marrow of each other 3 days after HLI. **(B)** Representative images of FACS analysis of the macrophage's percentage in the muscle tissue of WT and $Hdc^{-/-}$ mice transplanted with bone marrow of each other 3 days after HLI. **(C)** Volcano plot of the expression difference between ischemia muscle tissue of WT mice and $Hdc^{-/-}$ mice 3 days after HLI. Red dots indicate transcripts that were increased (padj< 0.05, Log2 fold change > 1), whereas blue dots indicate decreased transcripts (padj< 0.05, Log2 fold change < 1). **(D)** Heat map of the expression difference between ischemia muscle tissue of WT mice and $Hdc^{-/-}$ mice 3 days after HLI. **(E)** Venn diagram showing the common expression difference between sc-RNA-seq before and after HLI in WT mice and RNA-seq in WT mice and $Hdc^{-/-}$ mice 3 days after HLI. **(F)** Optical microscope image of M0 Macrophages, M1 Macrophages, and M2 Macrophages collected from bone marrow of WT and $Hdc^{-/-}$ mice; Scale bar, 50μm. **(G)** Elisa of secreted IL-1β, Il-6, VEGFA, and MMP-9 from BMDMs of WT and $Hdc^{-/-}$ mice. BMDMs were treated with LPS/IFN-γ or IL-4/IL-13 for 24 h (n=6). **(H)** Heat map showing KEGG enrichment analyses of ischemia muscle tissue of WT mice and $Hdc^{-/-}$ mice 3 days after HLI. **(I)** Heat map showing GO enrichment analyses, KEGG enrichment analyses and Wiki Pathway of five macrophage subtypes. For all experiments, error bars represent the mean ± SD.*P < 0.05, **P < 0.01, ***P < 0.001, ****P < 0.0001.

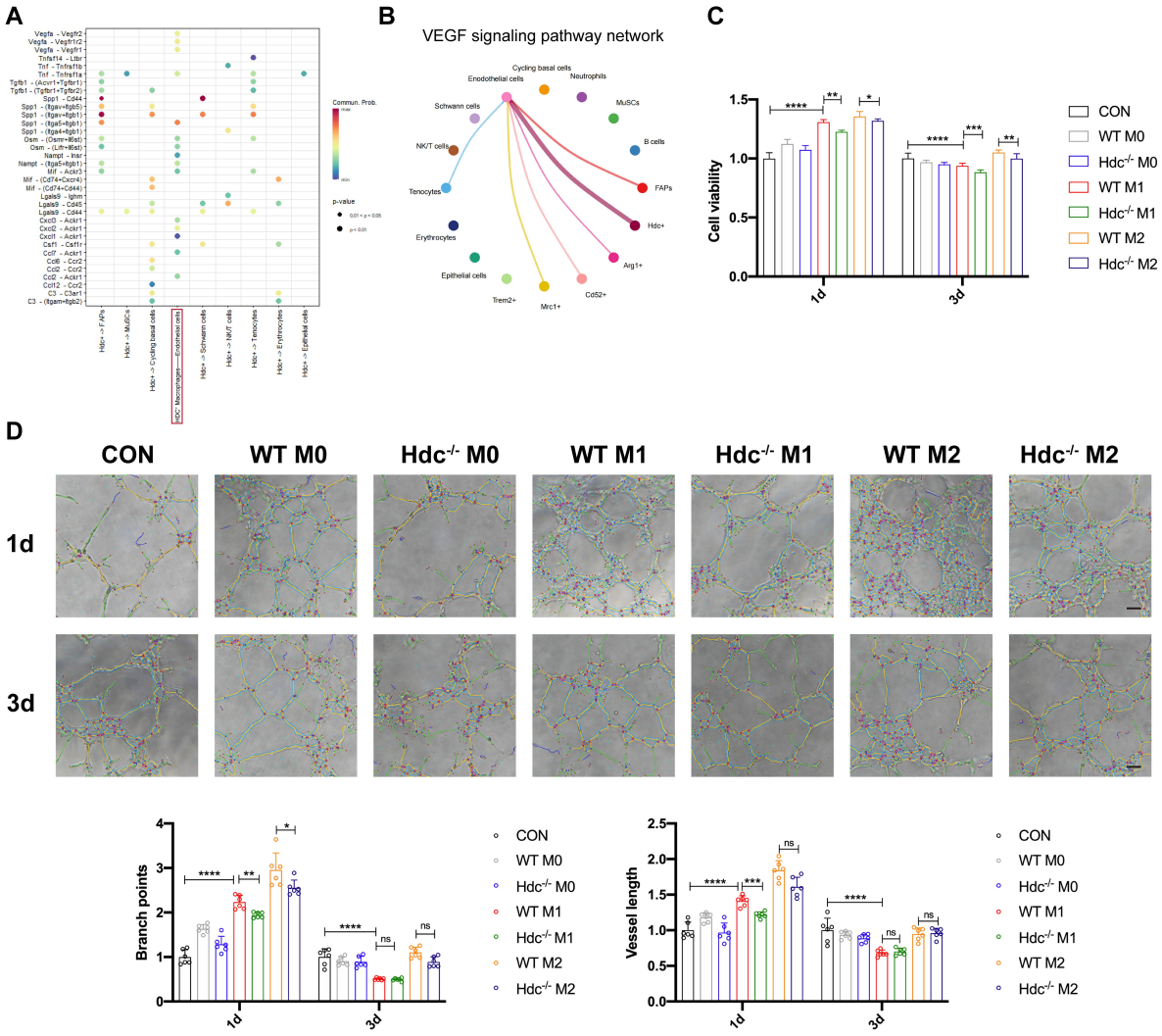

Fig. S5. HDC^{+} macrophages combine to endothelial cells via CXCR2-CXCL2 loop and promote angiogenesis mediated by VEGF, MMP-9, and IL-1β (A) Heatmap of HDC^{+} macrophage interacts with various types cells in skeletal muscle. **(B)** Cell chat showing HDC^{+} macrophage interacts with various types cells though VEGF in skeletal muscle. Edges are scaled by the inferred regulatory potential of the interaction. **(C)** CCK8 cell proliferation test of HUVECs co-cultured with WT BMDM and Hdc-/- BMDM for 1 day and 3 days. HUVECs were pretreated with 10μM H_2O_2 and 1μm AST; BMDMs were treated with LPS/IFN-γ or IL-4/IL-13

for 24 h; Scale bars, 50μm; (n=6). **(D)** Representative images and quantification of tube formation assay of HUVECs co-cultured with WT BMDM and $Hdc^{-/-}$ BMDM for 1day and 3days. HUVECs were pretreated with 10μM H_2O_2 and 1μm AST; BMDMs were treated with LPS/IFN-γ or IL-4/IL-13 for 24 h; Scale bars, 50μm; (n=6). For all experiments, error bars represent the mean ± SD.*P < 0.05, **P < 0.01, ***P < 0.001, ****P < 0.0001.

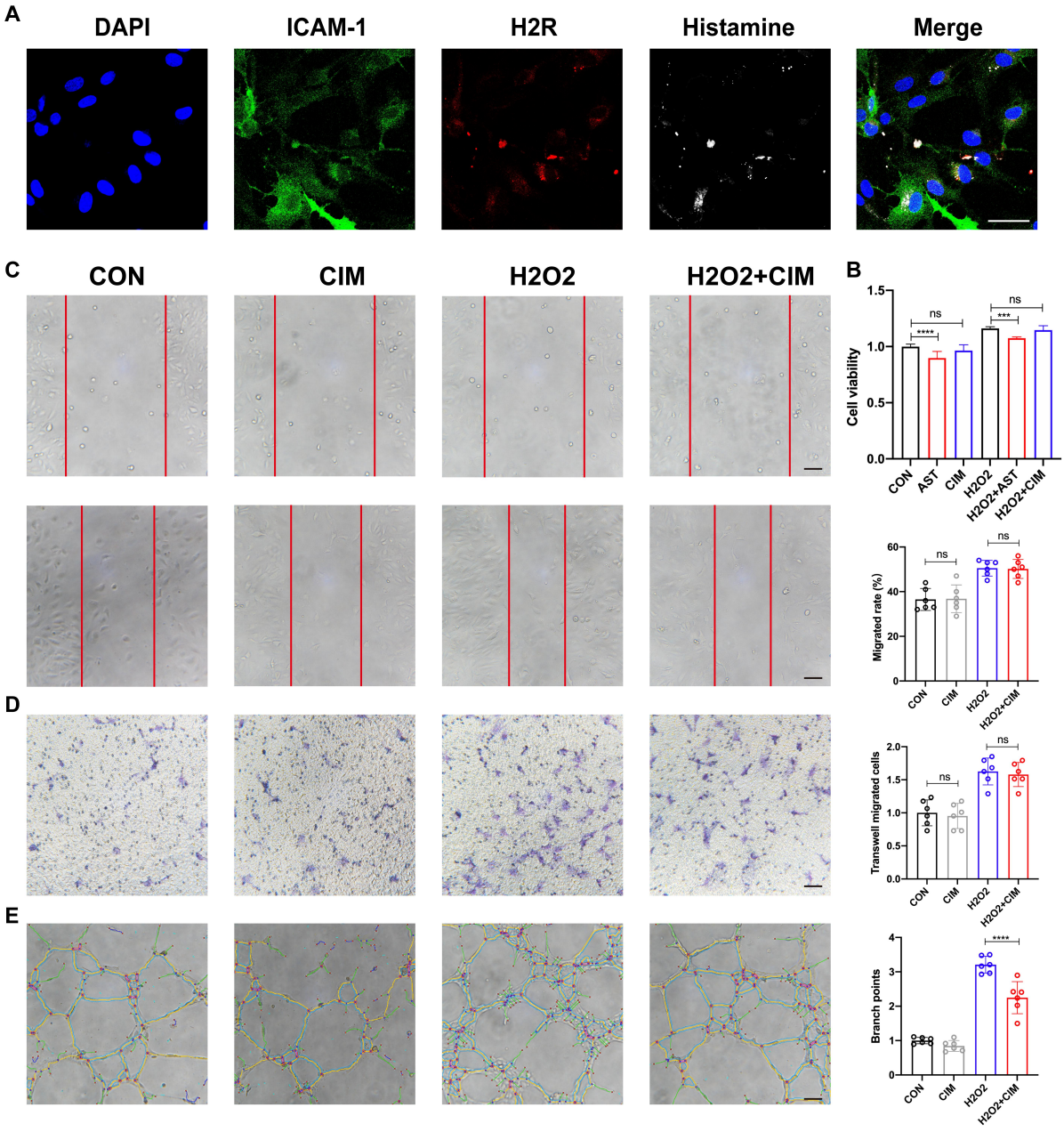

Fig. S6. Histamine promotes endothelial cell migration and tube formation by activating H_1R and CXCL/PI3K/AKT signaling pathway (A) Representative images of ICAM-1(green), H_2R (red), histamine (white) and DAPI (blue) immunostainings of HUVECs; scale bar, 20μm. **(B)** CCK8 cell proliferation test of HUVECs cultured in conditioned medium with or without 1μM AST or CIM. HUVECs were pretreated with 10μM H_2O_2. (n=6). **(C)** Representative

images and quantification of scratch wound healing assay of HUVECs cultured in conditioned medium with or without 1μM CIM. HUVECs were pretreated with 10μM H_2O_2. Scale bars, 50μm, (n=6). **(D)** Representative images and quantification of transwell assays of HUVECs cultured in conditioned medium with or without 1μM CIM. HUVECs were pretreated with 10μM H_2O_2. Scale bars, 50μm, (n=6). **(E)** Representative images and quantification of tube formation assay of HUVECs cultured in conditioned medium with or without 1μM CIM. HUVECs were pretreated with 10μM H_2O_2. Scale bars, 50 μm, (n=6). For all experiments,error bars represent the mean ± SD.*P < 0.05, **P < 0.01, ***P < 0.001, ****P < 0.000

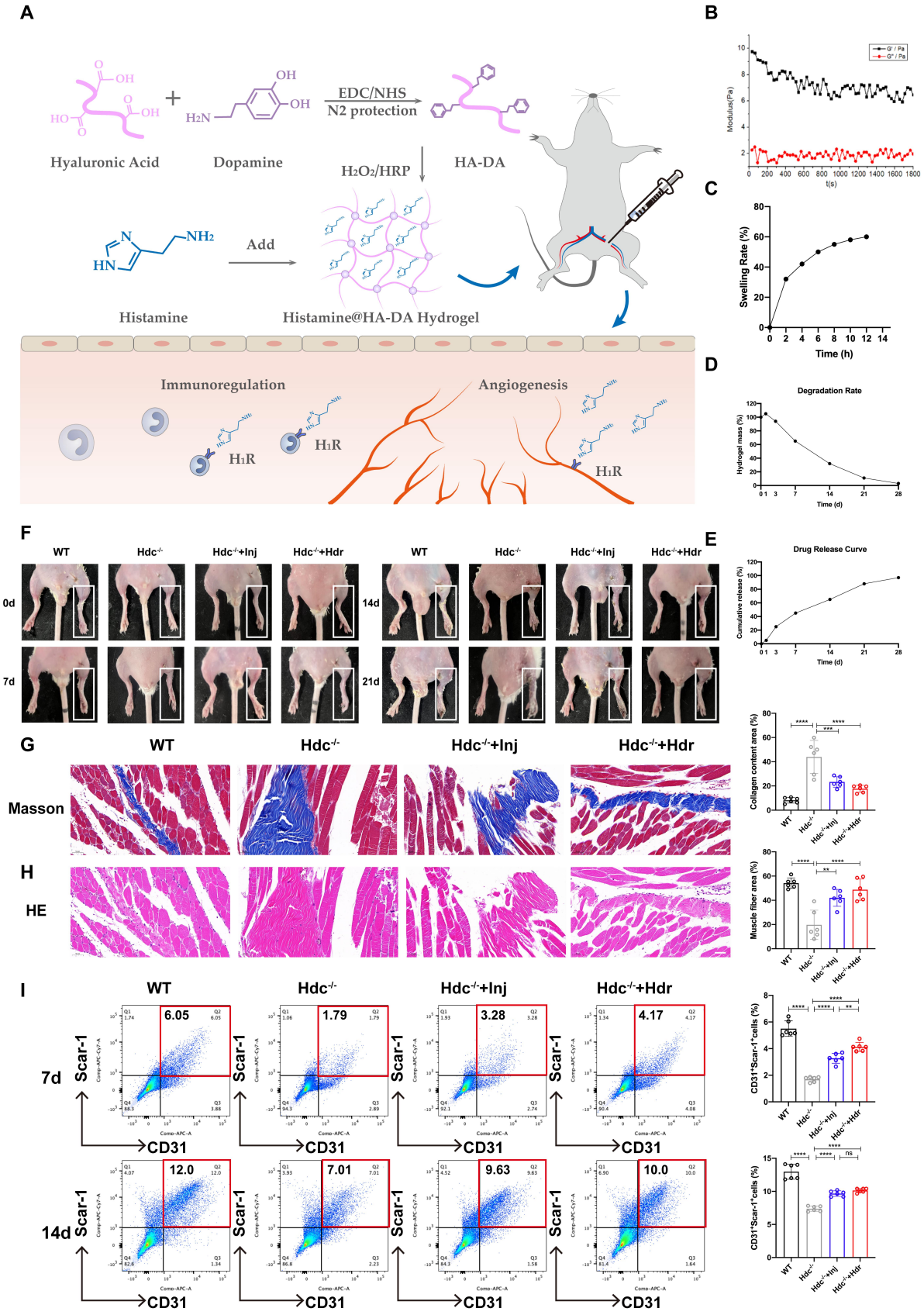
A
Hyaluronic Acid
Dopamine
EDC/NHS
N2 protection
HA-DA
H2O2/HRP
Histamine
Add
Histamine@HA-DA Hydrogel
Immunoregulation
Angiogenesis
H1R
B
Modulus(Pa)
t(s)
C
Swelling Rate (%)
Time (h)
D
Degradation Rate
Hydrogel mass (%)
Time (d)
E
Drug Release Curve
Cumulative release (%)
Time (d)
F
WT
Hdc-/-
Hdc-/-+Inj
Hdc-/-+Hdr
0d
7d
14d
21d
G
Masson
H
HE
Collagen content area (%)
Muscle fiber area (%)
I
7d
14d
Scar-1
CD31
6.05
1.79
3.28
4.17
12.0
7.01
9.63
10.0
CD31+Scar-1+cells (%)

1

Fig. S7. Histamine-delivering Hydrogel promotes skeletal muscle regeneration in Hdc$^{-/-}$ mice after HLI by regulating angiogenesis and inflammatory disorders (A) Schematic illustration on gene therapy strategy of HA-DA@histamine hydrogel or delivering histamine to ischemic limb to promote angiogenesis, reduce ischemia-induced muscle damage and restore limb function. **(B)** Rheological properties of HA-DA@histamine hydrogel at 37°C. **(C)** Swelling rate of HA-DA@histamine hydrogel at 37°C in PBS. **(D)** Degradation rate of HA-DA@histamine hydrogel at 37°C in PBS. **(E)** The release rate of histamine from HA-DA@histamine hydrogel at 37°C in PBS. **(F)** A picture of the ischemic limb is shown at each point per group. Each photograph was taken under the same conditions. **(G)** Representative images and quantitative analysis of Masson' s staining of injured gastrocnemius muscle from each group at day 21 post injury in ischemic muscles (n=6); Scale bar, 50μm. **(H)** Representative images and quantitative analysis of H&E staining of injured gastrocnemius muscle from each group at day 21 post-injury in ischemic muscles (n=6); Scale bar, 50μm. **(I)** Representative flow cytometry plots with quantification of $CD31^+$ $Sca\text{-}1^+$ endothelial cells (n=6). For all experiments, error bars represent the mean ± SD.*$P < 0.05$, **$P < 0.01$, ***$P < 0.001$, ****$P < 0.0001$.

Supplementary Tables

Table S1. Animals (in vivo studies)

Species	Vendor or Source	Background Strain
Wide type mice	Department of Laboratory Animal Science at Fudan University	Balb/C
$Hdc^{-/-}$ mice	Supplied by Professor Timothy C. Wang	Balb/C
Hdc-GFP mice	Supplied by Professor Timothy C. Wang	Balb/C

Table S2. Fluorochrome-conjugated antibodies used in flow cytometry analysis

Experiments	Antibodies	Cat No.	Company
Macrophage identification and polarization	CD45	147709	Biolegend
	CD11b	101211	Biolegend
	Ly6C	128018	Biolegend
	Ly6G	127616	Biolegend
	F4/80	123110	Biolegend
	CD86	374207	Biolegend
	CD206	321121	Biolegend
Endothelial cells and angiogenesis	CD31	102410	Biolegend
	Scar-1	108125	Biolegend

Table S3. Primary antibodies used in experiments

Experiments	Antibodies	Cat No.	Company
Immunofluorescence and	CD31	ab182981	Abcam
immunohistochemistry assay	CD68	ab283654	Abcam
	α-SMA	ab179467	Abcam
Western blot	CXCR-2	A3301	Abcronal
	ERK	#4695	Cell Signaling Technology
	p-ERK	#4370	Cell Signaling Technology
	iKBα	#4812	Cell Signaling Technology
	p-iKBα	#2859	Cell Signaling Technology
	PI3K(p85)	ab191606	Abcam
	AKT	#4691	Cell Signaling Technology
	p-AKT	#4060	Cell Signaling Technology

Table S4. Primary antibodies used in experiments

Gene	Sequence 5'-3'	Species
Gapdh	F: CCACTCACGGCAAATTCAAC R: GTAGACTCCACGACATACTCAG	*Mus musculus*
Hdc	F: TGCCTGTGTTTGTCTGTGCAACG R: ATCTGCCAATGCATGAAGTCCGTG	
H_1R	F: GCCTGGTTTCTCTCCTTCCT R: TGAGCAAAGTGGGGAGGTAG	
Il1β	F: ACTCATTGTGGCTGTGGAGA R: TTGTTCATCTCGGAGCCTGT	
Il6	F: CTGGGGATGTCTGTAGCTCA R: CTGTGAAGTCTCCTCTCCGG	
Arg-1	F: CTGAGCTTTGATGTCGACGG R: TCCTCTGCTGTCTTCCCAAG	
Mrc-1	F: TGGATGGATGGGAGCAAAGT R: GCTGCTGTTATGTCTCTGGC	
Vegfa	F: TCTCCTTCCTCTCTATTCACCT R: CATCCACCAGTCCATATACCTC	
Vegfb	F: CTATGACCGATTCCTGTCAGTC R: CGTGATGAGAAAGTACCAGTTG	
Mmp-9	F: TGGGCGTTAGGGACAGAAAT R: GAACCATAACGCACAGACCC	
Gapdh	F: GGCTGTTGTCATACTTCTCATGG R: GGCTGTTGTCATACTTCTCATGG	*Homo sapiens*
Hdc	F: ATGCACGCCTACTACCCAG R: CAGTCCATGACGTTCATCTCC	
H_1R	F: AGATGTGTGAGGGCAACAAGA R: CAAGCAGATAGTGCTCAGGAC	
Vcam-1	F: GGGAAGATGGTCGTGATCCTT R: TCTGGGGTGGTCTCGATTTTA	
Cxcl-1	F: ACTCTACCTGCACACTGTCC R: TCCCCTGCCTTCACAATGAT	
Cxcl-2	F: CGCCCAAACCGAAGTCATAG R: CTCTGCAGCTGTGTCTCTCT	
Cxcl-5	F: AGCTGCGTTGCGTTTGTTTAC R: TGGCGAACACTTGCAGATTAC	
Cxcl-9	F: CCAGTAGTGAGAAAGGGTCGC R: AGGGCTTGGGGCAAATTGTT	
Cxcl-10	F: GTGGCATTCAAGGAGTACCTC R: TGATGGCCTTCGATTCTGGATT	
Cxcl-12	F: ATTCTCAACACTCCAAACTGTGC R: ACTTTAGCTTCGGGTCAATGC	
Cxcl-13	F: GCTTGAGGTGTAGATGTGTCC R: CCCACGGGGCAAGATTTGAA	

Table S5. Result of Mendelian randomization (MR)

Outcome	Exposure	Method	nsnp	b	se	pval
	Ant-ihistamine medication	MR Egger	10	0.653251919	0.455050691	0.189049289
Sequel of lower limb injuries	Anti-histamine medication	Weighted median	10	0.466976953	0.195508223	0.016915998
Sequel of lower limb injuries	Anti-histamine medication	Inverse variance weighted	10	0.353664617	0.152956643	0.020767288
Sequel of lower limb injuries	Anti-histamine medication	Simple mode	10	0.4745811	0.3127703	0.163489992
Sequel of lower limb injuries	Anti-histamine medication	Weighted mode	10	0.500100985	0.310773482	0.142030465

Table S6. Horizontal pleiotropy tests of Mendelian randomization (MR)

Outcome	Exposure	egger_intercept	se	pval
Sequel of lower limb injuries	Anti-histamine medication	-0.025768518	0.036863073	0.504343372

Table S7. Pleiotropy test of Mendelian randomization (MR)

Outcome	Exposure	Method	Q	Q_df	Q_pval
Sequel of lower limb injuries	Anti-histamine medication	MR Egger	4.558602914	8	0.803541838
Sequel of lower limb injuries	Anit-ihistamine medication	Inverse variance weighted	5.047250567	9	0.830170001